A novel low-cost ZMP estimation method for humanoid gait using inertial measurement devices: Concept and experiments

Ratan Das, Ahmed Chemori, Neelesh Kumar

Preprint - International Journal of Humanoid Robotics

A NOVEL LOW-COST ZMP ESTIMATION METHOD FOR HUMANOID GAIT USING INERTIAL MEASUREMENT DEVICES: CONCEPT AND EXPERIMENTS

RATAN DAS

Academy of Scientific and Innovative Research (AcSIR), Ghaziabad-201002, India

CSIR-Central Scientific Instruments Organisation, Chandigarh, India, E-mail:ratans16@gmail.com

AHMED CHEMORI*

LIRMM, University of Montpellier, CNRS, Montpellier, France, E-mail: ahmed.chemori@lirmm.fr

NEELESH KUMAR

Academy of Scientific and Innovative Research (AcSIR), 201002, Ghaziabad, India

CSIR-Central Scientific Instruments Organisation,, Chandigarh, India, E-mail:neel5278@csio.res.in

Received
Revised

Estimation and control of Zero Moment Point (ZMP) is a widely used concept for planning the locomotion of bipedal robots and is commonly measured using integrated joint angle encoders and foot force sensors. Contemporary methods for ZMP measurement involve built-in contact sensors such as joint encoders or instrumented foot force sensors. This paper presents a novel approach for computing ZMP for a humanoid robot using inertial sensor-based wireless foot sensor modules (WFSM). The developed WFSMs, strapped at different limb segments of a bipedal robot, measure lower limb joint angles in real-time. The joint angle trajectories, further transformed into cartesian position coordinates, are used for estimating the ZMP positions of humanoid robots using the planar biped model. The whole framework is presented through experimental studies for different real-life walking scenarios. Since the modules work based on the limb motion and inclination, any ground unevenness would be automatically reflected in the module output. Hence, this measurement process can be a convenient method for applications requiring humanoid control on uneven surfaces/ outdoor terrains**.** To compare the performance of the proposed model, ZMP is simultaneously measured from inbuilt foot force sensors and joint encoders of the robot. Statistical tests exhibit a high linear correlation between the proposed method with integrated encoders and foot force sensors (Pearson's coefficient, $r > 0.99$). Results indicate that ZMP estimated by WFSM is a viable method to monitor the dynamic gait balance of a humanoid robot and has potential application in outdoor and uneven terrains.

Keywords: Bipedal locomotion; Inertial Measurement; Plantar Force; Support Polygon; Zero Moment Point

*Corresponding author

1. Introduction

Bipedal robots [1-3] and their application in various sectors is an important topic of current research. The goal of a bipedal locomotion control[4] is to provide mobility to perform the specified task efficiently. One major challenge towards this goal is ensuring balance and stability by compensating for any action that may lead to unrecoverable falling motion. It is a challenge owing to the number of Degrees of Freedom (DoF) of the robot and motion dynamics, including disturbances. One of the most widely adopted stability indicators for biped walking is Zero Moment Point (ZMP) [5-9]. ZMP specifies the point w.r.t. which the reaction force at the contact of the foot with the ground does not produce any moment in the horizontal direction. Furthermore, the behavior of all the forces acting on the mechanism can be replaced by a single force acting on that point. Walking is a cyclical and sequential activity with the repetition of single and double support phases and alteration of both legs. The double support phase is when both feet are in contact with the ground, and the overall system is mainly stable. As long as all the ground-sole contacts appear on a single plane surface, the Center of Pressure (CoP) and the ZMP are at the same point, called CoP-ZMP. Both these are two interpretations of the acting force-moment between the ground and the first link of a kinematic chain [10]. In the Honda biped robots, an application of the CoP-ZMP control has been implemented, showing that the CoP notion is related to contact forces, and that of the ZMP signifies the gravity plus inertia forces [11].

The dynamical postural stability of the robot is usually quantified by the distance between the ZMP and the boundaries of the polygon of support [12]. During the single support phase, only one leg is in contact with the ground, and this phase tends to be statistically less stable compared to the double support phase. Hence, the coordinates of ZMP trajectory during walking are determined by the positions of the single support leg, and the robot tends to be stable when the ZMP lies within the support polygon. [13] proposed a Dynamic Linear Inverted Pendulum Model (DLIPM) to plan the robot trajectory w.r.t. change in dynamic balance (signified by the ZMP) to minimize the control error and reduce robot oscillations. Similarly, [14] proposed a cascaded control approach for balance control in a terrain-blind environment. The first stage of the cascaded controller is a capture-point controller [15] that updates with a stable ZMP value that counters the disturbances. The adjusted ZMP acts as a reference to the second stage of the controller (a balance controller). This dynamic ZMP adjustment w.r.t. variation in terrains ensures a robust operation of the bipedal robot. A similar capture-point tracking controller that mainly targets updating the zero moment point for bipedal walking dynamically is also reported in [9, 15, 16].

The most prevalent ZMP estimation method is using foot pressure sensors and load cells [17-20]. However, such measurement systems may not be effective in case of uneven surfaces where apposite foot contact with the ground is not possible. [21] reviewed and outlined the force-torque sensor used in state-of-the-art humanoid robots for zero-moment point estimation and dynamic control. A traditional force-torque sensor-based ZMP measurement requires the sensor to be compact, lightweight, repeatable, and overload protection with particular consideration for impact [21]. Another important requirement for a foot force-based sensor is to ensure the measurement range is sufficient enough to account for any additional weights and the impact of the foot during ground contact [22]. In the case of running, the vertical ground reaction force generated during a foot contact or foot lift is twice that of body weight [23]. To protect the force sensors from damage resulting from the impact force,

robot foot soles need to be designed with impact-absorbing parts. As a result, different sizes of robots and applications that require carrying additional weights (service robots) will, in all likelihood, require customized sensing soles. Moreover, this technique requires the integration of force sensing modules in the robot foot, which may not always be available/feasible. Another alternative method to compute the ZMP is from the variation of different joint angles [24, 25]. In such technique, the robot is mainly modeled by an inverted pendulum system with simple joints and links [26-29]. The joint angles information, measured from integrated joint encoders, is used for calculating the Cartesian position coordinates of the robot. The moments of individual links are combined to synthesize the ZMP of the overall mechanism.

In the present work, we propose using our developed wireless foot sensor modules (WFSM) 30 to estimate the ZMP during various humanoid robot motions. The WFSM is a compact and low-power sensing system that measures 3-axis rotational angles (roll, pitch, and yaw) around any joint. The measured joint angles from the WFSM are acquired wirelessly using a tool developed in LabVIEW and further processed in real-time to compute the ZMP during the robot locomotion. The basic principle and detailed working of the developed WFSM system is discussed in the next section. The aim and contribution of the reported work are to experimentally validate the concept of ZMP measurements from joint kinematics, using developed wireless inertial modules for a bipedal gait. Since the WFSMs are strapped/mounted on the limbs rather than the foot insole, they don't alter the natural trajectory. Moreover, a WFSM weighs only 31 gm which can further be reduced with component integration. Moreover, in the present case, the contact impact has no mechanical effect on the WFSMs. As a result, the same approach can be extended for varying sizes/weights of bipedal robots. These modules can easily be strapped around a joint to measure the motion trajectory. They can be an extremely convenient method to compute the ZMP of bipedal systems with no built-in integrated foot sensors or encoders. Since a bipedal robot has a more demanding control requirement to maintain gait balance, the motion data recorded from these modules may further be used for balance and stability analysis of the robot. It is also a promising integration method for analyzing motions and ZMP evolution in scenarios involving outdoor applications and uneven terrains. Hence, these 'ready-to-strap' WFSMs present an alternate and viable solution to address the common challenges (as mentioned in the previous paragraph) associated with ZMP measurement using load cells or encoders.

The rest of the paper is organized as follows: The working of the developed wireless module and the kinematic model of the NAO humanoid robot are detailed in section 2. This section also elaborates on the mathematical formulation for ZMP measurements from WFSM, encoders, and FSRs. The trial and data collection scenarios are highlighted in the last part of the same section. Section 3 presents the results obtained by three different measurement methods for different walking scenarios. A comparative analysis of the measured ZMPs for all the measurement mentioned above methods and trial scenarios is also presented in the section's later part. The paper concludes by highlighting the contribution and significance of the ZMP estimation using inertial sensors and possible future application.

2. Material and methods

This reported work involves estimating ZMP for a humanoid robot walking from an inertial

sensor-based measurement system. Real-time joint angle data from WFSMs are acquired and processed accordingly to estimate the evolution of ZMP during humanoid gait under different scenarios. The principle and working of the proposed method along with the detailed experimental design are presented below.

2.1. Test and Measurement Platform

The developed WFSM is a compact, low-power, wireless device (cf. figure1) that provides a measure of joint angle trajectories. The authors in their previous work [30] have reported its application for measurement of foot angle during human gait and subsequently for estimating the gait events. The WFSM is used for measuring the value of accelerations and angular velocities along the x-axis (a_x and ω_x), the y-axis (a_y and ω_y), and z-axis (a_z and ω_z), respectively. The acceleration and angular velocity parameters are then used for computing the inclination angles. The gyro sensor estimates the angle (θ_{gyro}) by numeric integration of the angular velocity, that is

$$\omega = \frac{d\theta_{gyro}}{dt} \tag{1}$$

$$\theta_{gyro} = \int_0^t \omega . dt \approx \sum_0^t \omega(t) . T_s \tag{2}$$

where T_s is sampling time and ω is the angular rate. The accelerometer angle (θ_{acc}) is derived by computing the projection of the gravitation vector a_x, a_y and a_z as follows [31]

$$\theta_{acc} = \tan^{-1}\left[\frac{a_x}{\sqrt{{a_y}^2+{a_z}^2}}\right] \tag{3}$$

Two major errors that inertial sensors are prone to are error accumulation due to gyroscopic drift and vibrations in the accelerometer due to ground impact [32, 33]. Since the error is present in both systems, a complementary filter [34, 35] is implemented to compensate for the effects of the sensor's individual weaknesses. Such a method is often useful when two different measurement sources are used to estimate a single variable and the noise properties of these sources are such that one source shows high performance in the low-frequency region and the other gives valid results in the high-frequency region. This argument holds good for inertial sensors consisting of accelerometers and gyroscopes. The output angle of the complementary filter (θ_C) is expressed by (4) [34]

$$\theta_C = k \times (\theta_C + \theta_{gyro} \times dt) + (1 - k) \times \theta_{acc} \tag{4}$$

Here, k is the optimized complementary filter coefficient, and dt is the sampling time. The output angle from the complementary filter is the fusion of gyroscope and accelerometers. At high frequencies, the gyro angle dominates, and the resultant angle at low frequencies is compensated by the accelerometer angle (θ_{acc}) [36].

A humanoid robot can be resolved into a simplified links and joints model, where the torso, shank, and calf represent the different links. Control and measurement of joint angles play an important role in generating the motion trajectory and stability of the humanoid robot. The recorded joint angles are used to estimate the Cartesian position coordinates of different limb segments and joints, which can be used to estimate the ZMP.

Fig. 1. Developed Wireless Foot Sensor Module.

NAO is an autonomous humanoid robot (cf. figure 2) developed by Aldebaran Robotics, France and currently owned by Softbank Robotics, Japan. The robot can be programmed to perform numerous activities like walking, dance[37] and is even used for therapeutic applications [38]. It has various sensors like joint angle encoders, Force Sensitive Resistors (FSR), tactile and proximity sensors, cameras, and an inertial measurement unit [39]. The joint encoders measure the joint angle variation during any activity, including walking, while the FSRs give measurement of distributed weights acting on different foot points. The inertial unit, consisting of two axes gyroscope and a three axes accelerometer located at the torso of the NAO, is used for ascertaining the inclination of the robot in sagittal and transverse planes. The robot supports up to 25 DoF with access to each individual joint control.

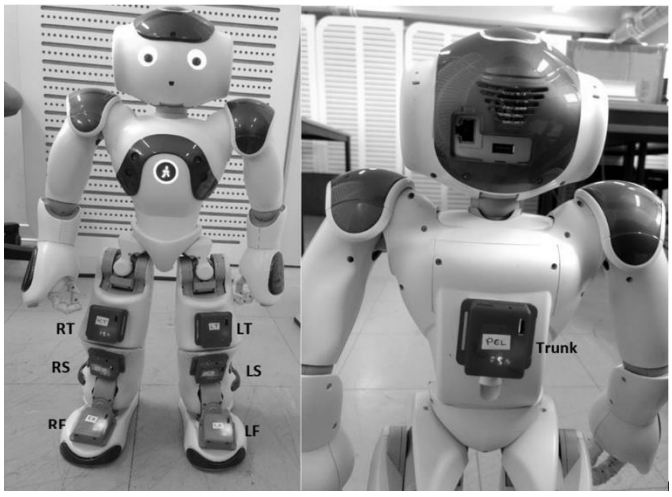

Fig. 2. Illustration of the placement of wireless inertial modules on NAO's body segments.

2.2. Calculation of ZMP

This section details the underlying principle of ZMP evaluation based on the three sensing techniques i.e., joint encoders, WFSMs and FSRs. For ZMP estimation based on built-in encoders, the humanoid robot is resolved into a planar biped model [3]. The WFSM-based ZMP estimation begins with measuring the lower limb joint angles of the robot and further

feeding the joint angles into the planar biped model. The foot force sensor-based method is a widely used concept of ZMP estimation based on the weight distribution in the foot.

2.2.1. Method 1: Using Joint Encoders

A biped robot is generally resolved into a five-link model (Figure 3). The ankle joint of the stance leg is considered the origin of the coordinate system. In this work, the walking is constrained in the sagittal plane, i.e. forward x-direction. The lengths and masses of different segments are summarized in Table 1. For a given set of joint angles, the Cartesian coordinates of a particular joint can be computed using polar coordinates transformation. Assume the coordinates of the left ankle (origin) are represented by (X_{la}, Y_{la}, Z_{la}), then the position of the left knee can be expressed as

$$X_{lk} = X_{la} + (calf_l \times \sin(LK)) \quad (5)$$

$$Z_{lk} = Z_{la} + (calf_l \times \cos(LK)) \quad (6)$$

$$Y_{lk} = X_{lk} \times Z_{lk} \quad (7)$$

Similarly, the point coordinates for the left hip (X_{lh}, Y_{lh}, Z_{lh}), the right hip (X_{rh}, Y_{rh}, Z_{rh}), the right knee (X_{rk}, Y_{rk}, Z_{rk}) and the right ankle (X_{ra}, Y_{ra}, Z_{ra}) can be calculated. The position of the overall ZMP of the robot can be expressed as follow [25]

$$ZMP_x = \frac{\sum_i m_i(\ddot{Z}_i+g)X_i - \sum_i m_i \ddot{X}_i Z_i}{\sum_i m_i(\ddot{Z}_i+g)} \quad (8)$$

$$ZMP_y = \frac{\sum_i m_i(\ddot{Z}_i+g)Y_i - \sum_i m_i \ddot{Y}_i Z_i}{\sum_i m_i(\ddot{Z}_i+g)} \quad (9)$$

where *m* corresponds to the mass of respective limb segment, *g* denotes the acceleration due to gravity, and *i* varies between 1-5, where i(1)=la, i(2)=lk, i(3)=rk, i(4)=la and i(5)= h.

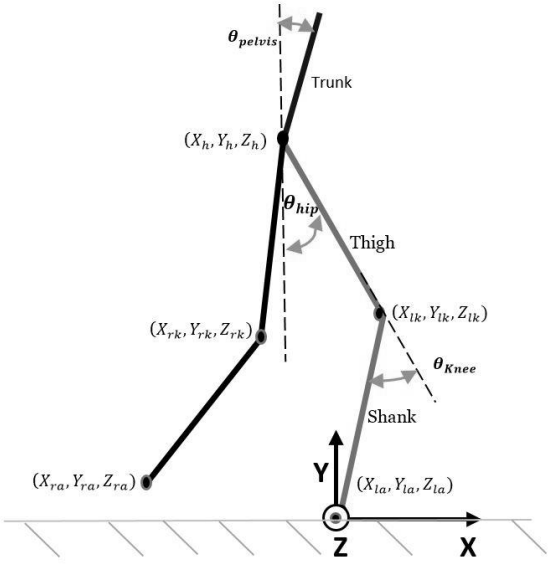

Fig. 3. Illustration of the planar biped model of the robot.

2.2.2. Method 2: Using WFSM

A WFSM is placed at the torso, thigh, calf, and foot, as illustrated in Figure 2-a, of the NAO robot to collect the variation of joint angles w.r.t. any posture/motion in real-time. An application is developed in LabVIEW for data acquisition, processing, and data logging. All the modules are synchronized using a digital trigger before the start of the trial and any offset angle associated are automatically zeroed from the software. All the joint angles (relative angles) are computed from the absolute angles measured from the WFSM modules as illustrated in Figure 2-b as follows

$$\theta_{Pelvis} = \theta_{trunk} \quad (10)$$

$$\theta_{hip} = \theta_{thigh} \quad (11)$$

$$\theta_{knee} = \theta_{shank} - \theta_{thigh} \quad (12)$$

$$\theta_{ankle} = 90 + \theta_{foot} - \theta_{knee} \quad (13)$$

Table 1: Physical dimensions of the joint segments of NAO robot

	Foot	**Shank**	**Thigh**	**Trunk**
Mass (kg)	0.17	0.29	0.39	1.74
Length (m)	0.04	0.10	0.10	0.21

The knee angle is computed as the difference of variation of the thigh and shank as any variation in the thigh brings in equal changes in the shank, even when there is no motion produced in the knee joint. Similarly, for foot motion, the variation in the ankle angle is measured as the difference of measurements from the foot module and knee angle. These angle measurements are further used to calculate the position coordinates of the NAO segment joints, and subsequently the ZMP by using the method explained above in section 2.2.1.

2.2.3. Method 3: Using Foot FSR

A simplified model for ZMP calculation based on plantar force variation is given in [40]. The position of the four FSRs under each foot is shown in Figure 4. The ZMP curve shifts alternatively towards the supporting leg during the swing phase of the contralateral foot. In this study, the left foot is considered the origin of the foot reference system as shown in Figure 4. The coordinates of all other FSRs including the right foot are obtained from the NAO technical specifications [39]. The stance leg ZMP equation, which also corresponds to the CoP is given by

$$X_{ZMP}(L) = \frac{F_1 x_1 - F_2 x_2}{F_1 + F_2} \quad (14)$$

$$Y_{ZMP}(L) = \frac{F_3 y_1 - F_4 y_2}{F_3 + F_4} \quad (15)$$

where F1, F2 are the sum of FSR values (in sagittal plane, and F3 and F4 are the sum of sensors in y-direction, that is $F_1 = f1 + f2$; $F_2 = f3 + f4$; $F_3 = f1 + f3$; $F_2 = f2 + f4$; and f1-f4 denotes the individual ground reaction forces recorded by different FSRs, as shown in Fig. 4b.

For the right foot, the coordinates of the FSRs and hence Y_{ZMP} is computed w.r.t. the origin of the left foot reference system considering the step width. For single-support phase, the overall ZMP of the system is described by the ZMP of the stance leg. With every alternative step, X_{ZMP} of the swing leg during next foot contact is incremented by the step length of the humanoid. The overall ZMP for the robot during the double support phase is given by averaging the sum of ZMP of both individual foot, that is

$$X_{ZMP} = \frac{X_{ZMP}(L)+X_{ZMP}(R)}{2} \tag{16}$$

$$Y_{ZMP} = \frac{Y_{ZMP}(L)+Y_{ZMP}(R)}{2} \tag{17}$$

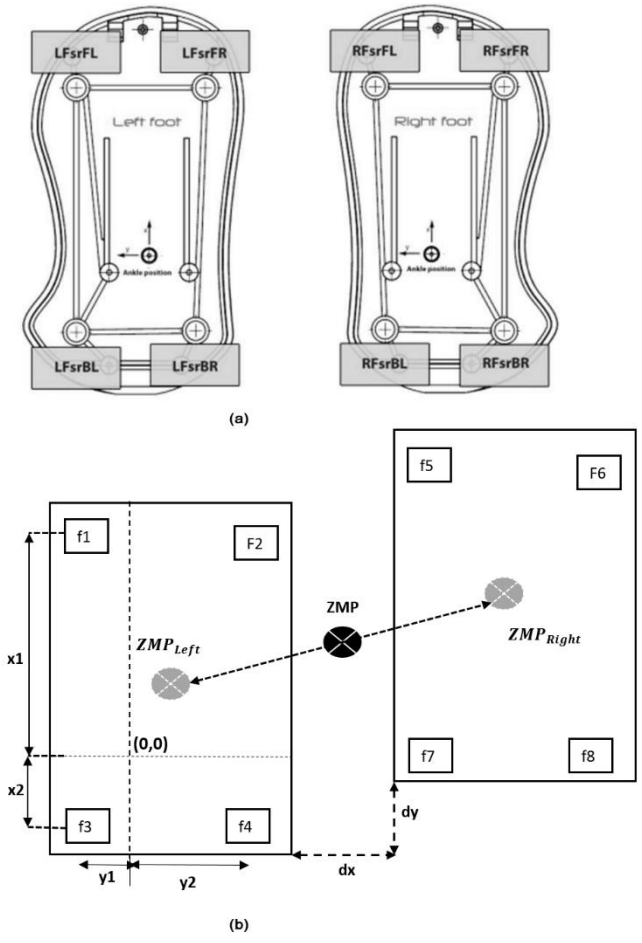

Fig. 4. (a) FSR position on NAO's feet (b) ZMP evolution during one step gait. Here dx denotes the step width and dy denotes the step length.

2.2.4. Trial Protocol

Walking patterns for the robot were generated for three different conditions: Straight line Walk (WS), Walk with Turn (WT) and Walk with added Weight (WW). For WS, the

humanoid robot is programmed to walk for approximately 1.5 meter in straight line and stop. The speed of the robot is set at default with a maximum step length of 0.08 meters. During WT, the NAO walks straight (x-direction) and then takes a 180º turn towards left and walk towards the direction of origin. Figure 5-a & 5-b illustrates the direction of progression of the NAO robot during WS and WT, respectively. For WW, a block of 250 gm was strapped to forearm of the NAO (as shown in figure 5-c) and it followed the same protocol as WS.

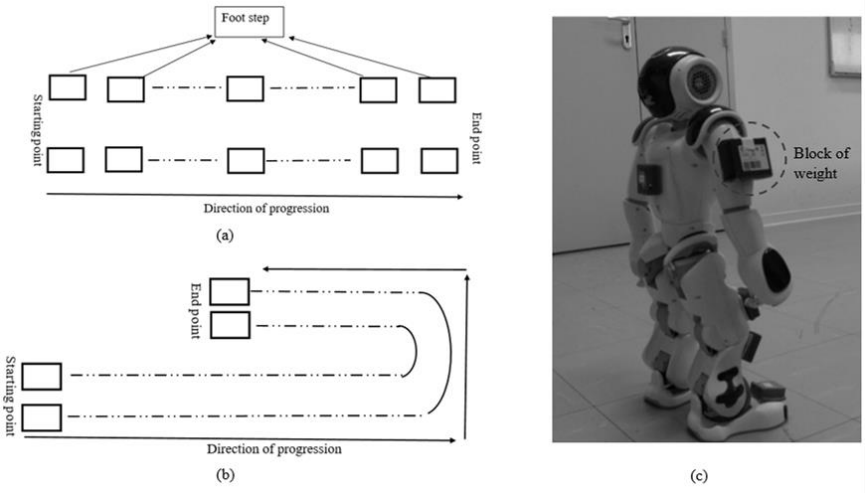

Fig. 5. (a) NAO trajectory for WS scenario (b) Direction of progression for WT scenario (c) the encircled portion shows the extra block of weight added to the NAO right arm

3. Results

All joint angle trajectories are recorded from the integrated NAO encoders and WFSMs simultaneously during the robot motion at a rate of 20Hz. Figure 6 shows the comparison of the right thigh angle, measured during straight walk, using WFSM and NAO encoder.

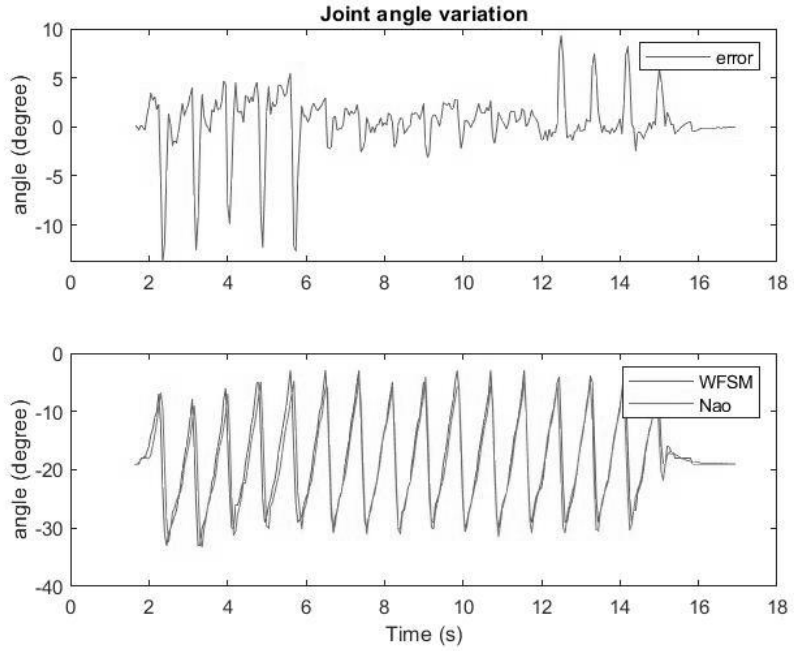

Fig. 6. Comparison of right Thigh angle vs Time as measured from encoder and WFSMs.

The FSRs based measurement is well-established method for computing ZMP of humanoids and thus, in this study, is considered as the ground truth for comparing the ZMP results estimated from joint encoders and WFSMs. Figure 7 displays the ZMP support area (Y-ZMP vs. X-ZMP) for the straight walk as computed from FSRs. This figure illustrates the ZMP evolution during transition of the foot from single support to double support phase to single support of the contralateral foot.

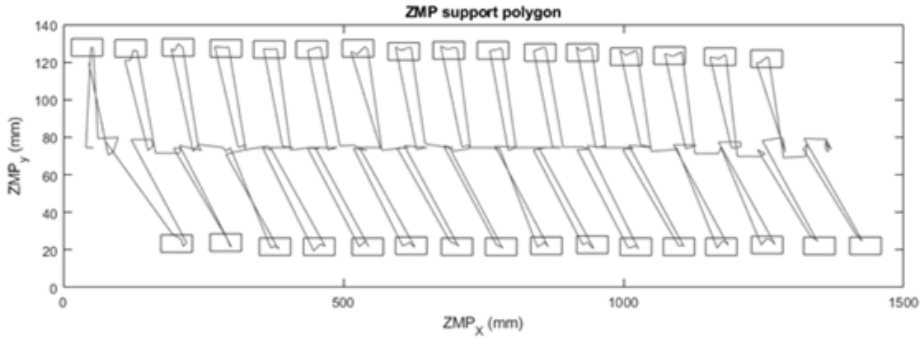

Fig. 7. Evolution of the ZMP support area measured from FSRs.

The comparison of the ZMP during the 'Walk Straight' protocol is presented in Figure 8. For ZMP progression along X-axis, the error (mean±SD) calculated using WFSMs and NAO encoders is -94±44 mm and -142±37 mm, respectively. The mean error reported between the two joint angle based ZMP calculation is 47±21 mm. Figure 9 depicts the ZMP (normalized) along Y-axis for the same trial. The average ZMP along Y-axis is about 123±2

mm, 116±3 and 74±32 mm as computed from encoders, WFSMs and FSRs, respectively.

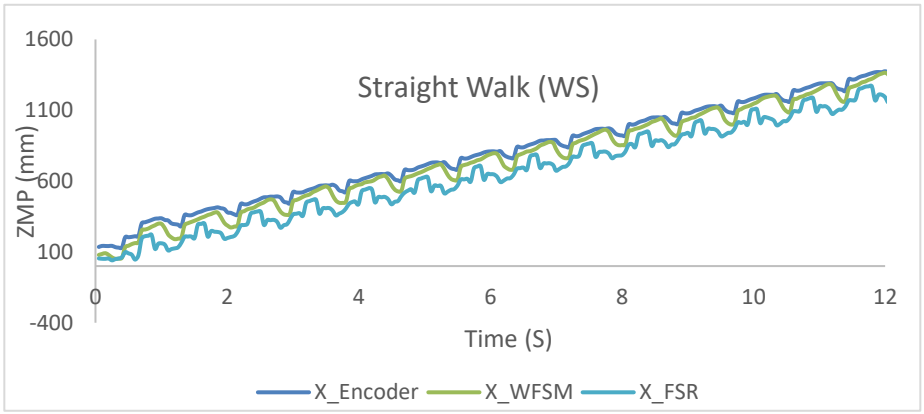

Fig. 8. Evolution of ZMP versus time along x-axis during the straight walking scenarios.

Similarly, the error reported for X-ZMP with WFSM, NAO encoders during Walk and Turn is around 52±20 mm, and Walk with added weight is 52±34 mm, which is roughly equivalent to that of error reported during straight walk. A Bland-Altman plot for WW protocol showed the mean bias ± standard deviation (SD) between encoder and WFSM measurements for X-ZMP as 52.6 ± 34.96 cm, and the limits of agreement were −15.92 and 121.13 mm (Figure 11).

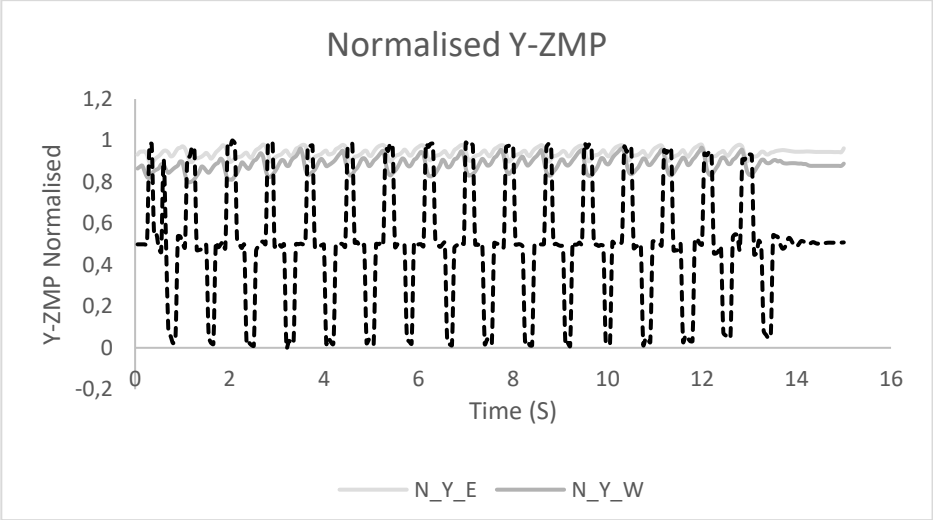

Fig. 9. Evolution vs. time of the normalized ZMP along y-axis during straight walk scenarios.

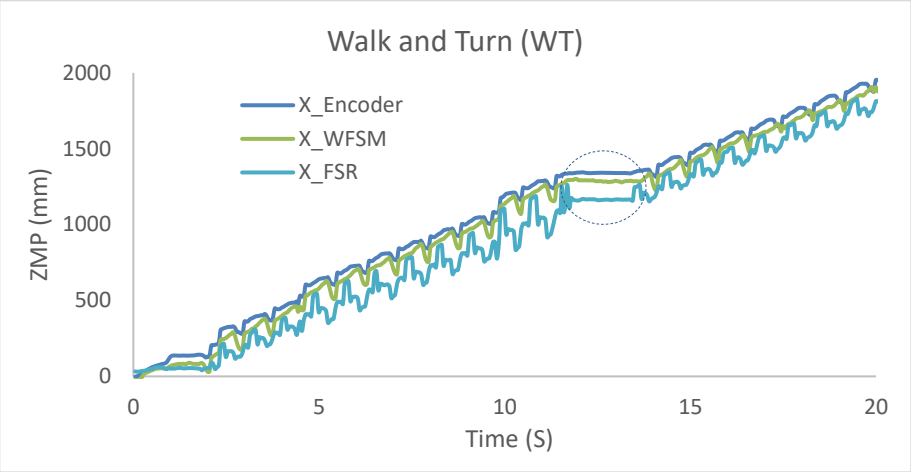

Fig. 10. Evolution of the ZMPx position versus time during walking with turn protocol.

As pointed out previously, the ZMP analysis in this work is done along the sagittal plane i.e. x-axis. During the time when the robot takes a turn, it sweeps a little distance in the lateral side. However, there is insignificant change in the joint angles and hence ZMP in direction of forward progression. This phase is pointed out in the encircled area in figure 10, where there is negligible progression along x-axis. To draw the correlation between the three measurement methods, Pearson's correlation coefficient (r) was computed for all three walk protocols. The estimated ZMP from WFSMs exhibited high degree of correlation with measured ZMP for WS (r =0.9967), WT (r = 0.9994) and WW (r = 0.9881) using encoders, and WS (r =0.9942), WT (r = 0.9943) and WW (r = 0.9854) using FSRs. This signifies that the proposed measurement technique can be explored for dynamic walking balance analysis, even with constrained protocols/background.

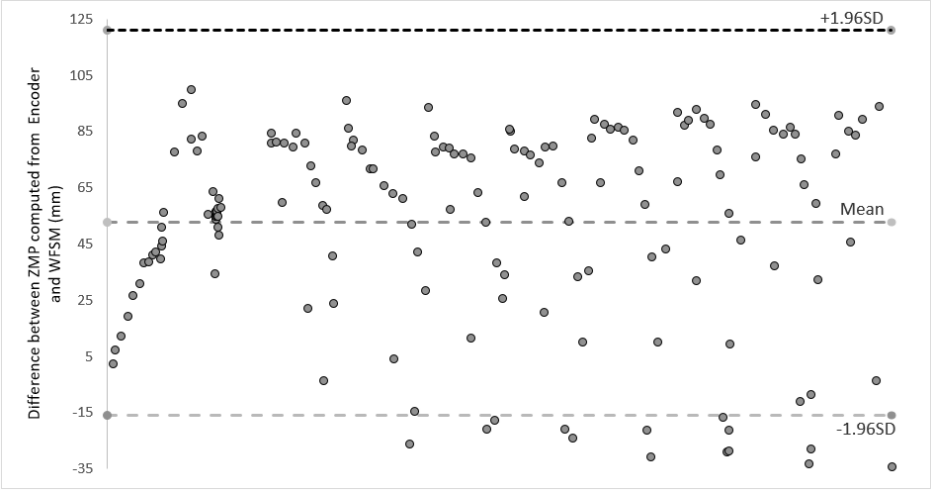

Fig. 11. Bland-Altman plot showing the limits of agreement between the proposed WFSM and joint encoder based ZMP evaluation method for X-ZMP during WW protocol.

4. Conclusions and Future Work

ZMP is one of the most important aspect for maintaining balance and stability during bipedal walking. This work experimentally validates a method for ZMP estimation of a bipedal robot using wireless inertial sensor modules. These modules are light in weight (~31gms), low cost (~INR 1500) and has wireless data transmission capability. The WFSM modules records the joint trajectories of limb segments, which are further used to compute the position coordinates. Experiments shows that the proposed method can effectively be used for ZMP estimation of bipedal walk even under certain constraints like unbalanced weight distribution. One main distinct advantage the proposed WFSM based ZMP estimation possesses over force-torque sensor based measurement is its capability to be strapped to the body (rather than beneath the foot). Owing to lightweight, easy to integrate and wireless data communication features, the same can easily be adopted to different situations without altering/affecting the pre-existing setups. This also shows a promising alternate to overcome certain challenges associated with a traditional foot-torque based sensor like stringent placement requirement, additional cushioning and customized solution for robots with varying shape and size. These factors make it suitable, for instance, for application in situations that require controlling a biped robot in an uneven surface or outside laboratory constraint. The real time approach of the proposed estimation method makes it promising alternate for effective response to emergency situations like fall. Moreover, the WFSM based measurements has tremendous potential for healthcare applications, especially towards fall detection in elderly. Gait imbalance and tendency of fall are very common in older age causing serious accidents and injuries. There are reported work for fall detection and prevention based on ZMP and CoP based measurements [41-43]. The authors are working towards extending the work towards human gait balance assessment and envisages the use of WFSMs as a simple and reliable tool for postural balance assessment.

Declarations

Funding: This study was funded by IFCPAR/CEFIPRA, New Delhi, India, project grant no. DST CNRS 2016-03

Conflicts of interest/Competing interests: The authors declare that they have no conflict of interest.

Availability of data and material:

The data that support the findings of this study are openly available in Mendley at https://data.mendeley.com/datasets/p8frdzcc5h/1 [DOI: 10.17632/p8frdzcc5h.1].

Acknowledgements

The authors are thankful to IFCPAR/CEFIPRA, New Delhi, for supporting this work through their Indo- French bilateral project grant. R. Das acknowledges the support of UGC, India, for supporting his PhD through its national fellowship programme.

References

1. Hirose M. and Ogawa K. 2007, "Honda humanoid robots development," *Philosophical Transactions of the Royal Society A: Mathematical, Physical and Engineering Sciences* **365**, 11-19.
2. Adams B., Breazeal C., Brooks R. A. and Scassellati B. 2000, "Humanoid robots: A new kind of tool," *IEEE Intelligent Systems and Their Applications* **15**, 25-31.
3. Chemori A. and Alamir M. 2006, "Multi-step limit cycle generation for Rabbit's walking based on a nonlinear low dimensional predictive control scheme," *Mechatronics* **16**, 259-277.
4. Kuffner J. J., Kagami S., Nishiwaki K., Inaba M. and Inoue H. 2002, "Dynamically-stable motion planning for humanoid robots," *Autonomous robots* **12**, 105-118.
5. Vukobratović M. and Borovac B. 2004, "Zero-moment point—thirty five years of its life," *International journal of humanoid robotics* **1**, 157-173.
6. Vukobratovic M. and Juricic D. 1969, "Contribution to the synthesis of biped gait," *IEEE Transactions on Biomedical Engineering*, 1-6.
7. Kim J.-Y., Park I.-W. and Oh J.-H. 2007, "Walking control algorithm of biped humanoid robot on uneven and inclined floor," *Journal of Intelligent and Robotic Systems* **48**, 457-484.
8. Goswami A. 1999, "Postural stability of biped robots and the foot-rotation indicator (FRI) point," *The International Journal of Robotics Research* **18**, 523-533.
9. Kim I.-S., Han Y.-J. and Hong Y.-D. 2019, "Stability control for dynamic walking of bipedal robot with real-time capture point trajectory optimization," *Journal of Intelligent & Robotic Systems* **96**, 345-361.
10. Sardain P. and Bessonnet G. 2004, "Forces acting on a biped robot. Center of pressure-zero moment point," *IEEE Transactions on Systems, Man, and Cybernetics-Part A: Systems and Humans* **34**, 630-637.
11. Hirai K., Hirose M., Haikawa Y. and Takenaka T. 1998, "The development of Honda humanoid robot," in Proceedings. 1998 IEEE International Conference on Robotics and Automation (Cat. No. 98CH36146), ed.^eds. Editior (IEEE, pp. IEEE.
12. Jia Y., Luo X., Han B., Liang G., Zhao J. and Zhao Y. 2018, "Stability criterion for dynamic gaits of quadruped robot," *Applied Sciences* **8**, 2381.
13. Martinez S., Garcia-Haro J. M., Victores J. G., Jardon A. and Balaguer C. 2018, "Experimental robot model adjustments based on force–torque sensor information," *Sensors* **18**, 836.
14. Joe H.-M. and Oh J.-H. 2019, "A robust balance-control framework for the terrain-blind bipedal walking of a humanoid robot on unknown and uneven terrain," *Sensors* **19**, 4194.
15. Hong Y.-D. 2019, "Capture point-based controller using real-time zero moment point manipulation for stable bipedal walking in human environment," *Sensors* **19**, 3407.
16. Joe H.-M. and Oh J.-H. 2018, "Balance recovery through model predictive control based on capture point dynamics for biped walking robot," *Robotics and Autonomous Systems* **105**, 1-10.
17. Wee T.-C., Astolfi A. and Ming X. 2013, "The design and control of a bipedal robot with sensory feedback," *International Journal of Advanced Robotic Systems* **10**, 277.
18. S¸ afak K. K. and Baturalp T. B. 2010, "Design and analysis of a foot contact sensor for posture control of a biped robot," in Engineering Systems Design and Analysis, ed.^eds. Editior.

19. Baturalp T. B. 2010, "Design and analysis of a foot contact sensor for posture control of a biped robot," in ASME 2010 10th Biennial Conference on Engineering Systems Design and Analysis, ed.^eds. Editior (American Society of Mechanical Engineers Digital Collection, pp. American Society of Mechanical Engineers Digital Collection.
20. Sardain P. and Bessonnet G. 2004, "Zero moment point-measurements from a human walker wearing robot feet as shoes," *IEEE Transactions on Systems, Man, and Cybernetics-Part A: Systems and Humans* **34**, 638-648.
21. Kim J.-H. 2019, "Multi-Axis Force-Torque Sensors for Measuring Zero-Moment Point in Humanoid Robots: A Review," *IEEE Sensors Journal* **20**, 1126-1141.
22. Nishiwaki K., Kagami S., Kuniyoshi Y., Inaba M. and Inoue H. 2002, "Toe joints that enhance bipedal and fullbody motion of humanoid robots," in Proceedings 2002 IEEE International Conference on Robotics and Automation (Cat. No. 02CH37292), ed.^eds. Editior (IEEE, pp. IEEE.
23. Ngoh K. J.-H., Gouwanda D., Gopalai A. A. and Chong Y. Z. 2018, "Estimation of vertical ground reaction force during running using neural network model and uniaxial accelerometer," *Journal of biomechanics* **76**, 269-273.
24. Chen C.-P., Chen J.-Y., Huang C.-K., Lu J.-C. and Lin P.-C. 2015, "Sensor data fusion for body state estimation in a bipedal robot and its feedback control application for stable walking," *Sensors* **15**, 4925-4946.
25. Zhang X., Wang H., Shi Y., Fu C., Wang H. and Wang G. 2016, "A measure system of zero moment point using wearable inertial sensors," *China Communications* **13**, 16-27.
26. Mousavi P. N. and Bagheri A. 2007, "Mathematical simulation of a seven link biped robot on various surfaces and ZMP considerations," *Applied Mathematical Modelling* **31**, 18-37.
27. Sugihara T., Nakamura Y. and Inoue H. 2002, "Real-time humanoid motion generation through ZMP manipulation based on inverted pendulum control," in Proceedings 2002 IEEE International Conference on Robotics and Automation (Cat. No. 02CH37292), ed.^eds. Editior (IEEE, pp. IEEE.
28. Kajita S., Morisawa M., Miura K., Nakaoka S. i., Harada K., Kaneko K., Kanehiro F. and Yokoi K. 2010, "Biped walking stabilization based on linear inverted pendulum tracking," in 2010 IEEE/RSJ International Conference on Intelligent Robots and Systems, ed.^eds. Editior (IEEE, pp. IEEE.
29. Ragusila V. and Emami M. R. 2016, "Mechatronics by analogy and application to legged locomotion," *Mechatronics* **35**, 173-191.
30. Das R., Hooda N. and Kumar N. 2019, "A Novel Approach for Real-Time Gait Events Detection Using Developed Wireless Foot Sensor Module," *IEEE Sensors Letters* **3**, 1-4.
31. Fisher C. J. 2010, "Using an accelerometer for inclination sensing," *AN-1057, Application note, Analog Devices*, 1-8.
32. Alonge F., Cucco E., D'Ippolito F. and Pulizzotto A. 2014, "The use of accelerometers and gyroscopes to estimate hip and knee angles on gait analysis," *Sensors* **14**, 8430-8446.
33. Luinge H. J. and Veltink P. H. 2004, "Inclination measurement of human movement using a 3-D accelerometer with autocalibration," *IEEE Transactions on neural systems and rehabilitation engineering* **12**, 112-121.
34. Ariffin N. H., Arsad N. and Bais B. 2016, "Low cost MEMS gyroscope and accelerometer implementation without Kalman Filter for angle estimation," in Advances in Electrical, Electronic and Systems Engineering (ICAEES), International Conference on, ed.^eds. Editior (IEEE, pp. IEEE.

35. Kok M., Hol J. D. and Schön T. B. 2017, "Using inertial sensors for position and orientation estimation," *Foundations and Trends in Signal Processing* **11**, 1-153.
36. Chang H.-C., Hsu Y.-L., Yang S.-C., Lin J.-C. and Wu Z.-H. 2016, "A Wearable Inertial Measurement System With Complementary Filter for Gait Analysis of Patients With Stroke or Parkinson's Disease," *IEEE Access* **4**, 8442-8453.
37. Suzuki R., Lee J. and Rudovic O. 2017, "Nao-dance therapy for children with ASD," in Proceedings of the Companion of the 2017 ACM/IEEE International Conference on Human-Robot Interaction, ed.^eds. Editior.
38. Csala E., Németh G. and Zainko C. 2012, "Application of the NAO humanoid robot in the treatment of marrow-transplanted children," in 2012 IEEE 3rd International Conference on Cognitive Infocommunications (CogInfoCom), ed.^eds. Editior (IEEE, pp. IEEE.
39. Keloth S. M., Arjunan S. P., Raghav S., Kumar D. K. J. J. o. N. and Rehabilitation 2021, "Muscle activation strategies of people with early-stage Parkinson's during walking," **18**, 1-15.
40. Shaari N. L. A., Razali M. R. B., Miskon M. and Isa I. S. M. 2013, "Parameter study of stable walking gaits for NAO humanoid robot," *International Journal of Research in Engineering and Technology (IJRET)* **2**.
41. Li M., Xu G., He B., Ma X. and Xie J. 2018, "Pre-impact fall detection based on a modified zero moment point criterion using data from Kinect sensors," *IEEE Sensors Journal* **18**, 5522-5531.
42. Lee C. M., Park J., Park S. and Kim C. H. 2019, "Fall-Detection Algorithm Using Plantar Pressure and Acceleration Data," *International Journal of Precision Engineering and Manufacturing*, 1-13.
43. Di P., Huang J., Nakagawa S., Sekiyama K. and Fukuda T. 2013, "Fall detection and prevention in the elderly based on the ZMP stability control," in 2013 IEEE Workshop on Advanced Robotics and its Social Impacts, ed.^eds. Editior (IEEE, pp. IEEE.

Author biography

Ratan Das has received Ph.D. (Engineering Sciences) from the Academy of Scientific and Innovative Research (AcSIR), Ghaziabad-201002, India, and is working as a Research Fellow at CSIR-Central Scientific Instruments Organisation, Chandigarh, India. He received M.Tech. in Electronics Design and Technology from Tezpur Central University, India. His area of research includes wearable sensor development for gait analysis and wearable assistive robotics. He was a visiting Doctoral fellow at LIRMM, Montpellier,

Ahmed Chemori received the M.Sc. and Ph.D. degrees both in automatic control from the Polytechnic Institute of Grenoble, Grenoble, France, in 2001 and 2005, respectively. During 2004–2005, he was a Research and Teaching Assistant with the Laboratoire de Signaux et Systames and the University Paris 11. Then, he joined Gipsa-Lab as a CNRS Postdoctoral Researcher. He is currently a tenured Research Scientist working on automatic control and robotics with the French National Center for Scientific Research (CNRS), Montpellier Laboratory of Computer Science, Robotics, and Microelectronics, Montpellier, France. His research interests include nonlinear (adaptive and predictive) control and their real-time applications in different fields of robotics (underwater robotics, underactuated robotics, parallel robotics, humanoid robotics, and wearable robotic.

Neelesh Kumar is working as Sr. Principal Scientist in the Biomedical Instrumentation Unit of CSIR-Central Scientific Instruments Organisation Chandigarh since 2001. He is also serving as Professor at the Academy of Scientific and Innovative Research (AcSIR), Ghaziabad, India. He completed his Ph.D. in Gait analysis for Prosthetic development in 2012. He worked on projects of national importance like “Jai Vigyan” Linear Accelerator, Functional Electrical Stimulation System for Paraplegics, Electronics Portal Imaging System, and Electronic Knee Joint. Presently he is working on the development of Exoskeleton Devices for gait rehabilitation. His areas of interest are techniques of gait assessment, sensor development, design and development of assistive devices, and methods to quantify rehabilitation.